LOCAL-GATE ELECTRICAL ACTUATION, DETECTION, AND TUNING OF ATOMIC-LAYER MoS_2 NANOELECTROMECHANICAL RESONATORS

Rui Yang[1], Changyao Chen[2], Jaesung Lee[1], David A. Czaplewski[2] and Philip X.-L. Feng[1*]*
[1]Department of Electrical Engineering & Computer Science, Case School of Engineering, Case Western Reserve University, Cleveland, OH 44106, USA
[2]Center for Nanoscale Materials, Argonne National Laboratory, Argonne, IL 60439, USA

ABSTRACT

We report on the first single- and few-layer molybdenum disulfide (MoS_2) nanoelectromechanical resonators with local electrical gate, and the demonstration of *local-gate all-electrical* actuation, detection, and tuning of the atomic-layer MoS_2 resonators at very high frequency (VHF). These local-gate structures make MoS_2 vibrating-channel transistors (VCTs), and facilitate efficient frequency modulation (FM) electrical readout and local-gate resonance tuning of individual VCTs. The resonant responses are also verified by optical motion detection techniques. We have scaled down the dimensions of these VCTs to length (L) of 800 nm and air gap (g) of 170 nm in the suspended MoS_2 region, attaining fundamental-mode resonance frequency (f_0) up to 130 MHz, and local-gate electrical tuning up to $\Delta f_0/f_0 \approx 13\%$. The layer numbers of these MoS_2 devices are confirmed by their unique Raman and photoluminescence (PL) signatures. These local-gate devices establish the foundation for *all-electrical* readout of MoS_2 resonators and their arrays, toward *multiplexing* of *individually addressable* devices, which could enable arraying and large-scale integration of atomic-layer resonant systems for parallel signal transduction and resonance-based sensing.

INTRODUCTION

Atomically thin semiconducting crystals possess intriguing properties not observed in their bulk, such as thickness-dependent and strain-tunable band structures [1,2]. In nanoelectromechanical systems (NEMS), these two-dimensional (2D) semiconductors are typically in the membrane limit due to the ultrasmall thickness [3], which makes it possible to achieve scaled device with high frequency while having broad frequency tunability through strain engineering. They also provide high sensitivity due to their ultrasmall mass and large surface-to-volume ratio. These 2D semiconductors have an intrinsic bandgap, which allows them to form field-effect transistors (FETs) with high I_{on}/I_{off} ratios [4], and they could form VCTs when they are suspended because the conductance changes with the gate voltage. While graphene NEMS [5], including local-gate graphene resonators [6], and MoS_2 resonators [3,7-9] have been demonstrated, single- and few-layer MoS_2 NEMS resonators with local-gate actuation and electrical detection have not yet been explored. Here we demonstrate MoS_2 VCTs with local-gate configuration, with electrical actuation, detection, and local-gate electrical tuning of the nanomechanical resonances. When assembled into large-scale arrays, the local-gate structure would allow us to individually access and control these MoS_2 VCTs and their arrays, toward functional devices and complex systems.

FABRICATION

A representative doubly-clamped bi-layer (2L) MoS_2 VCT is shown in Fig. 1a and 1b, with the MoS_2 contacting the source (S) / drain (D) electrodes and suspended over the local gate (LG). The suspended region has length (L) of only 800 nm, which should lead to high resonance frequency. The depth profile is measured with a stylus profilometer (Fig. 1c), showing that the initial air gap (g_0) is ~170 nm. The illustration in Fig. 1d shows that the MoS_2 is on top of the S/D contacts, and the LG electrode is deposited on SiO_2 which makes it isolated from the underlying Si and enables local-gate control. To confirm the thicknesses of the MoS_2, we perform PL and Raman measurements [10,11]. Figure 1e and 1f show the PL and Raman spectra for the 2L device.

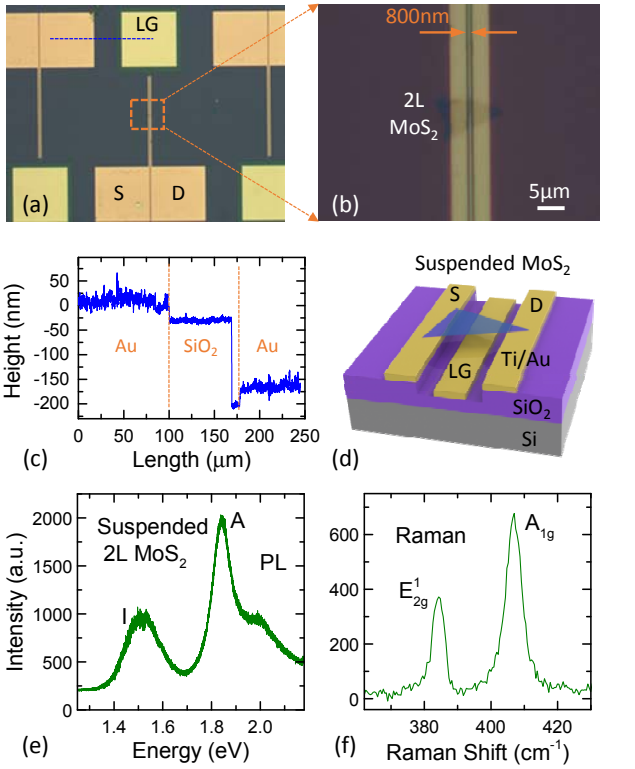

Figure 1: Local-gate MoS_2 VCT devices. (a) Optical image of a local-gate 2L MoS_2 VCT suspended over a rectangular microtrench. (b) Zoom-in optical image. (c) Depth profile of the dashed blue line in (a). (d) 3D-illustration of local-gate MoS_2 VCTs. (e) PL & (f) Raman spectra of the 2L MoS_2 in (b), measured in the suspended region.

The fabrication of the device starts from electron-beam lithography (EBL) on the 300 nm SiO_2/Si substrate followed by dry etching of the SiO_2 for ~170 nm to form the microtrenches (Fig. 2a). Then EBL is performed again with precise alignment to pattern the S/D electrodes, and then the LG electrodes (Fig. 2b). Evaporation of 5 nm Ti and 20 nm Au is then performed, followed by lift-off, to form the electrodes (Fig. 2c). MoS_2 is then dry-transferred onto the microtrench [12] (Fig. 2d). During the dry-transfer process, MoS_2 flakes are mechanically exfoliated onto a Nitto tape and then onto the PDMS stamp, and then the thin flakes are identified under an optical microscope via optical contrast. The MoS_2 flake is transferred with precise alignment onto the microtrenches using an XYZ stage. The device is then annealed in vacuum at 250ºC for 1 hour to improve the contact and remove possible surface adsorbates.

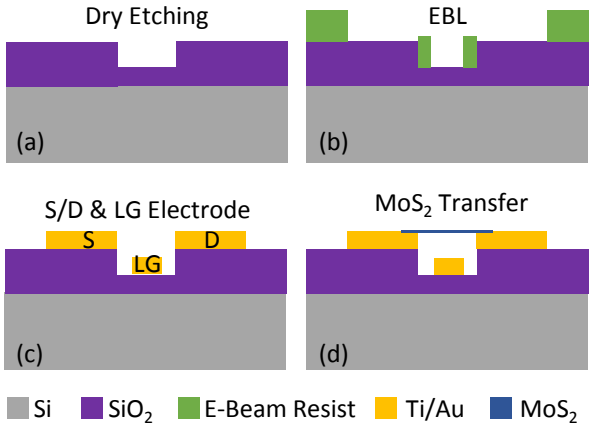

Figure 2: Fabrication process of the local-gate MoS_2 VCTs. (a) Dry etching on the 300 nm SiO_2/Si substrate, which etches through 170 nm SiO_2. (b) EBL to pattern the S/D, and then the LG electrode. (c) Metal (Ti 5 nm / Au 20 nm) evaporation and lift-off. (d) Dry-transfer of MoS_2 over the microtrench and vacuum thermal annealing.

RESULTS AND DISCUSSIONS

We measure the DC characteristics of these local-gate MoS_2 VCTs to make sure they have adequate electrical properties for resonance measurements (Fig. 4). During the measurement, the LG and D electrodes are connected to the source measurement units (SMUs) on a semiconductor parameter analyzer (Keithley 4200 SCS), while the S is grounded. The transfer characteristics (I_{DS}-V_{GS}) are shown in Fig. 3a, showing n-type conduction and high I_{on}/I_{off} ratio. I_{DS}-V_{DS} characteristics in Fig. 3b are not perfectly linear, but the current is enough for the resonance measurement.

We then perform FM mixing measurement on the devices, using the configuration shown in Fig. 4a. The function generator produces a frequency-modulated RF signal that is connected to the drain electrode, and the signal mixes with the device vibration-induced conductance change, and results in a low-frequency (LF) signal at f_L that is measured by the lock-in amplifier (LIA) [13]. A signal at f_L is also used as the reference of the LIA. A gate voltage (V_G) is applied at LG electrode to tune the channel conductance and the resonance frequency. The device is driven capacitively by the DC and RF voltages between the LG and S/D electrodes, which result in flexural-mode vibrations. The measurements are performed in moderate vacuum (~20 mTorr) and at room temperature (300K).

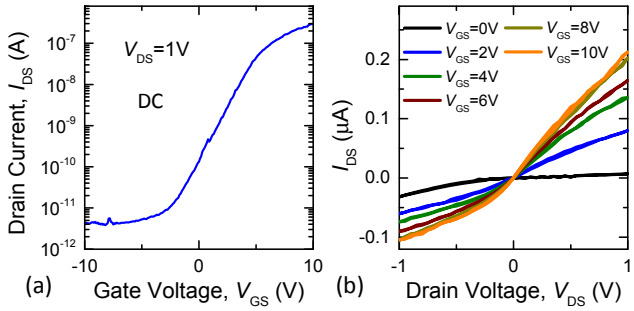

Figure 3: DC measurements of the 2L MoS_2 VCT shown in Fig. 1a and 1b. (a) I_{DS}-V_{GS} curve of the device measured at V_{DS}=1V. (b) I_{DS}-V_{DS} curves measured with varying V_{GS}.

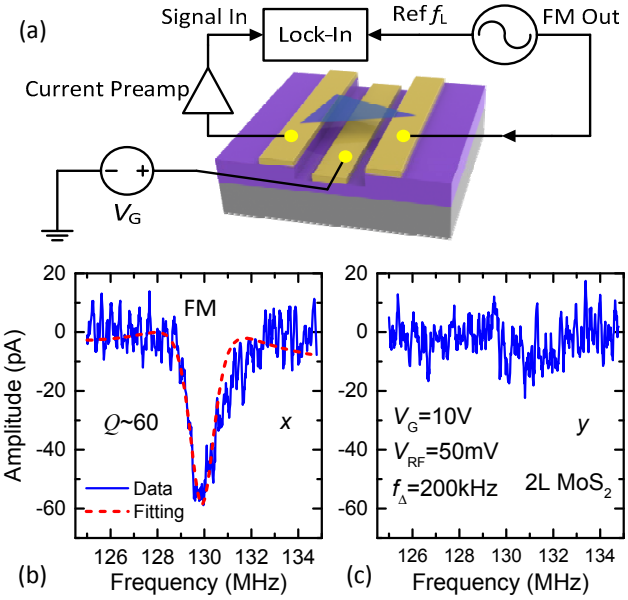

Figure 4: Frequency modulation (FM) mixing measurement of the local-gate MoS_2 VCTs. (a) Illustration of the FM mixing measurement setup. (b) & (c) FM mixing current of the 2L MoS_2 VCT shown in Fig. 1a and 1b, measured using reference frequency f_L=1 kHz, showing (b) in-phase and (c) out-of-phase current versus carrier frequency f_C.

Figure 4b and 4c show the measured FM mixing resonance of the same 2L MoS_2 device in Fig. 1a and 1b. The measured in-phase current (x) shows a clear fundamental-mode electromechanical resonance at f_0=130 MHz (Fig. 3c), with minimal out-of-phase current (y) (Fig. 3d). We perform fitting to the in-phase current and obtain a quality (Q) factor of Q ~ 60 for this device [8].

Tuning of the resonance frequency by the local gate voltage is also measured for these MoS_2 VCTs. Optical image of a device with the suspended region being a folded single-layer (1L) MoS_2 is shown in Fig. 5a. We measure V_G tuning of f_0 using the FM mixing signal (Fig. 5b), and show that f_0 is tuned up with increasing $|V_G|$. The tuning is due to

MoS_2 deflection induced by V_G, and for doubly-clamped membrane, the deflection induces additional strain in the channel. The device resonance frequency is given by

$$f_0 = \frac{1}{2L}\sqrt{\frac{\varepsilon E_{Y2D}}{\rho\alpha}}, \quad (1)$$

where ρ is the 2D mass density, α is adsorbed mass coefficient, ε is the total strain, E_{Y2D} is the 2D Young's modulus. With additional strain, ε increases, leading to a larger resonance frequency, increasing by up to ~3% for this folded 1L device. The tuning range in this device is mainly limited by the gate voltage we can apply to avoid leakage (through the SiO_2) and pull-in of the membrane.

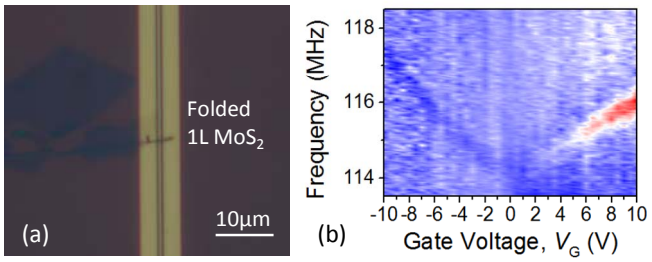

Figure 5: Measurements of a folded 1L MoS_2 VCT. (a) Optical image of the device. (b) In-phase mixing current amplitude in color scale versus V_G and f_C.

We also measure the resonance with ultrasensitive optical interferometry techniques to cross-check the resonance frequency (Fig. 6a), for the 1L MoS_2 VCT device shown in Fig. 5. The measurement system is similar to the one we previously employed for 6H-SiC resonators [14,15], except that here we use a 532 nm laser for interferometry.

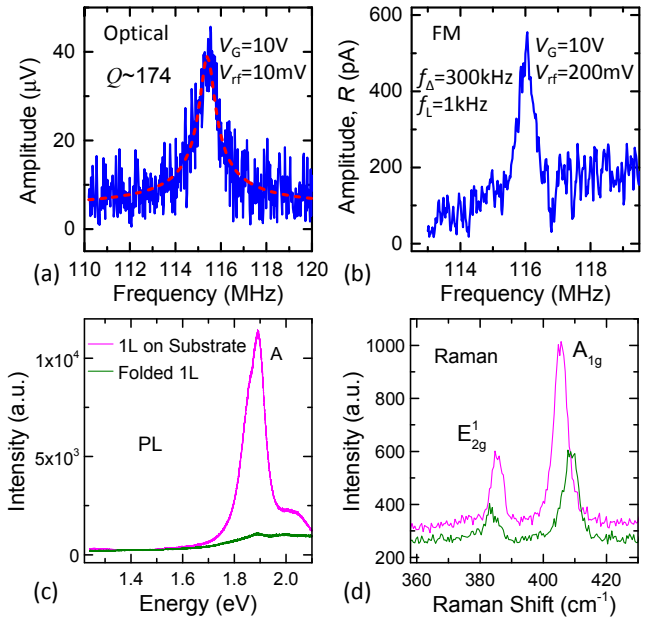

Figure 6: Characterization of the folded 1L MoS_2 VCT shown in Fig. 5a. (a) Electrically driven resonance measured using optical interferometry readout. (b) FM mixing current magnitude (R). (c) PL and (d) Raman spectra of the MoS_2 measured on substrate and in the suspended region.

During optical interferometry measurement, we drive the device capacitively by applying both DC and RF voltages to the LG electrode through a bias-tee, and grounding the S/D. At V_G=10V, we measure resonance at 115.5 MHz using laser interferometry (Fig. 6a), which is similar to the 116 MHz resonance measured with FM mixing (Fig. 6b). Fitting the optically measured resonance yields a Q~174. The magnitude (R) of the FM mixing signal is shown in Fig. 6b.

The same 532 nm laser is used for Raman and PL measurements, as shown in Fig. 6c and 6d. Because the suspended region is folded 1L MoS_2, the PL signal at the suspended region is quenched compared with the substrate-supported region without folding. For MoS_2 on SiO_2 substrate, we observe in PL the direct transition peak (A) with high intensity (Fig. 6c) without the indirect transition peak (I) as in the 2L device in Fig. 1e, confirming that the flake is 1L MoS_2 [10]. This is also verified by the Raman peak separation of 19.6 cm^{-1} at the substrate supported region, which corresponds to 1L MoS_2 [11], and it changes to 25.2 cm^{-1} for the folded suspended region.

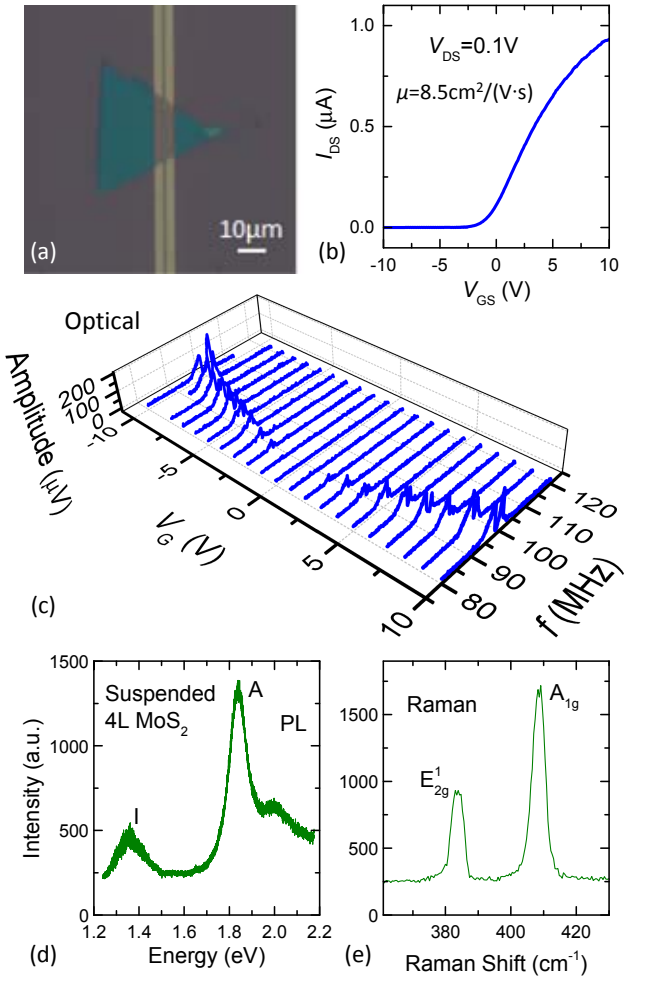

Figure 7: Characterization of a 4-layer (4L) MoS_2 VCT. (a) Optical image of the device. (b) I_{DS}-V_{GS} curve of the device measured in air, showing mobility (μ) of ~8.5 $cm^2/(V{\cdot}s)$. (c) Resonances measured with optical interferometry at different V_G. (d) PL and (e) Raman spectra of the suspended MoS_2.

Another thicker MoS_2 VCT device is measured to

determine the effect of thickness on device performance. The device also has doubly-clamped structure as shown in Fig. 7a, and the DC transfer characteristic shows n-type conduction (Fig. 7b). The resonances of this device are first measured using laser interferometry (Fig. 7c). By changing the LG voltage from -10V to 10V, we observe tuning of resonance frequency from 87 to 98 MHz, *i.e.*, $\Delta f_0/f_0 \approx 13\%$. We measure the PL and Raman spectra of the suspended MoS_2, and from the PL I peak position and Raman peak separation (~24.8 cm^{-1}), we infer that the MoS_2 is 4L thick.

FM mixing measurement is also performed on this 4L MoS_2 VCT. Figure 8 shows FM mixing resonance measured at LG voltage V_G=10V, and the in-phase mixing current (x) shows a dip on resonance, similar to that observed in Fig. 4b. The out-of-phase mixing current (y) shows minimal signal. Fitting the in-phase current signal shows a Q~130, and fundamental-mode resonance frequency f_0=101 MHz. The frequency deviation f_Δ is carefully chosen at 200 kHz to obtain clear mixing signal while measuring the correct Q [8]. Thicker MoS_2 has smaller bandgap and typically forms better contact to metal than single-layer MoS_2 does, resulting in better conductance and signal-to-noise ratio in resonance response. The technique is versatile and can be extended to various 2D semiconductors with different thicknesses.

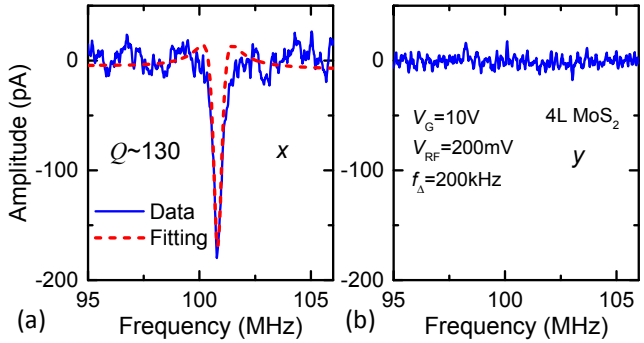

Figure 8: FM mixing measurement of the 4L MoS_2 VCT shown in Fig. 7a. (a) In-phase (x) and (b) out-of-phase (y) FM mixing current measured at reference frequency f_L=1 kHz. Fitting the in-phase resonance results in Q~130.

CONCLUSIONS

In summary, we have demonstrated local-gate single- and few-layer MoS_2 NEMS resonators. They are scaled down to 800 nm length and 170 nm air gap, with f_0 up to 130MHz. We show actuation, detection, and tuning of the device resonances using the local electrical gate, with frequency tuning of ~13% for the fundamental-mode resonance. The resonances are measured by using both FM mixing and optical interferometry techniques to confirm their NEMS nature. The thickness of the MoS_2 is identified by optical contrast and verified with Raman and PL signatures. These local-gate devices enable effective electrical detection with smaller parasitic capacitance, and can lead to on-chip electronic readout at RF through further engineering. Once integrated into an array, these devices can be individually addressable, and will be suitable for large-scale integration toward signal processing and sensing applications.

ACKNOWLEDGEMENTS

We thank the support from National Academy of Engineering (NAE) Grainger Foundation Frontier of Engineering (FOE) Award (FOE 2013-005), the National Science Foundation CAREER Award (ECCS-1454570). Use of the Center for Nanoscale Materials at the Argonne National Laboratory was supported by the U.S. Department of Energy, Office of Science, Office of Basic Energy Sciences, under Contract No. DE-AC02-06CH11357.

REFERENCES

[1] Q. H. Wang, *et al.*, "Electronics and Optoelectronics of Two-Dimensional Transition Metal Dichalcogenides", *Nature Nanotechnology*, vol. 7, pp. 699-712, 2012.

[2] R. Ganatra, *et al.*, "Few-Layer MoS_2: A Promising Layered Semiconductor", *ACS Nano*, vol. 8, pp. 4074-4099, 2014.

[3] J. Lee, *et al.*, "High Frequency MoS_2 Nanomechanical Resonators", *ACS Nano*, vol. 7, pp. 6086-6091, 2013.

[4] B. Radisavljevic, *et al.*, "Single-Layer MoS_2 Transistors", *Nature Nanotechnology*, vol. 6, pp. 147-150, 2011.

[5] C. Chen, *et al.*, "Performance of Monolayer Graphene Nanomechanical Resonators with Electrical Readout", *Nature Nanotechnology*, vol. 4, pp. 861-867, 2009.

[6] Y. Xu, *et al.*, "Radio Frequency Electrical Transduction of Graphene Mechanical Resonators", *Applied Physics Letters*, vol. 97, 243111, 2010.

[7] R. Yang, *et al.*, "Two-Dimensional MoS_2 Nanomechanical Resonators Freely-Suspended on Microtrenches on Flexible Substrate", in *Proc. 28th IEEE Int. Conf. on MEMS (MEMS 2015)*, pp. 877-880, Estoril, Portugal, January 18-22, 2015.

[8] R. Yang, *et al.*, "All-Electrical Readout of Atomically-Thin MoS_2 Nanoelectromechanical Resonators in the VHF Band", in *Proc. 29th IEEE Int. Conf. on MEMS (MEMS 2016)*, pp. 59-62, Shanghai, China, January 24-28, 2016.

[9] R. Yang, *et al.*, "Electromechanical Coupling and Design Considerations in Single-Layer MoS_2 Suspended-Channel Transistors and Resonators", *Nanoscale*, vol. 7, pp. 19921-19929, 2015.

[10] K. F. Mak, *et al.*, "Atomically Thin MoS_2: A New Direct-Gap Semiconductor", *Physical Review Letters*, vol. 105, 136805, 2010.

[11] C. Lee, *et al.*, "Anomalous Lattice Vibrations of Single- and Few-Layer MoS_2", *ACS Nano*, vol. 4, pp. 2695-2700, 2010.

[12] R. Yang, *et al.*, "Multilayer MoS_2 Transistors Enabled by a Facile Dry-Transfer Technique and Thermal Annealing", *Journal of Vacuum Science & Technology B*, vol. 32, 061203, 2014.

[13] V. Gouttenoire, *et al.*, "Digital and FM Demodulation of a Doubly Clamped Single-Walled Carbon-Nanotube Oscillator: Towards a Nanotube Cell Phone", *Small*, vol. 6, pp. 1060-1065, 2010.

[14] R. Yang, *et al.*, "6H-SiC Microdisk Torsional Resonators in a 'Smart-Cut' Technology", *Applied Physics Letters*, vol. 104, 091906, 2014.

[15] R. Yang, *et al.*, "Smart-Cut 6H-Silicon Carbide (SiC) Microdisk Torsional Resonators with Sensitive Photon Radiation Detection", in *Proc. 27th IEEE Int. Conf. on MEMS (MEMS 2014)*, pp. 793-796, San Francisco, CA, USA, January 26-30, 2014.

CONTACTS

*Emails: rui.yang@case.edu; philip.feng@case.edu